JOURNAL OF VIROLOGY, July 1992, p. 4364–4376
0022-538X/92/074364-13$02.00/0
Copyright © 1992, American Society for Microbiology
Vol. 66, No. 7

Conservation of RNA-Protein Interactions among Picornaviruses

SANDRA L. DILDINE AND BERT L. SEMLER*

Department of Microbiology and Molecular Genetics, College of Medicine, University of California, Irvine, California 92717

Received 2 January 1992/Accepted 2 April 1992

Picornavirus genomes encode unique 5′ noncoding regions (5′ NCRs) which are ~600 to 1,300 nucleotides in length, contain multiple upstream AUG codons, and display the ability to form extensive secondary structures. A number of recent reports have shown that picornavirus 5′ NCRs are able to facilitate cap-independent internal initiation of translation. This mechanism of translation occurs in the absence of viral gene products, suggesting that the host cell contains the necessary components for the cap-independent internal initiation of translation of picornavirus RNAs as well as cellular mRNAs. In an attempt to identify some of the perhaps novel cellular proteins involved in this newly discovered mechanism of translation, we utilized RNA mobility shift assays to identify and characterize interactions that occur between the 5′ NCR of poliovirus type 1 (PV1) and cellular proteins. In this report, we describe two separate interactions between RNA structures from the 5′ NCR of PV1 and proteins present in extracts from HeLa cells as well as other cell types. We describe the interaction between nucleotides 186 to 220 (stem-loop D) and a cellular protein(s) present in HeLa cell extracts. Mutational analysis of this stem-loop structure suggests that maintenance of a base-paired structure in the lower stem is necessary to present the sequences which directly interact with the protein(s). We also describe the interaction between nucleotides 220 to 460 (stem-loop E) and a cellular protein present in HeLa cell extracts. This RNA binding activity fractionates to a specific ammonium sulfate fraction (A cut) of a ribosomal salt wash. Mutational analysis of the stem-loop E structure suggests that the preservation of an extensive RNA structure is necessary for a strong interaction with the cellular protein(s), although smaller RNAs derived from this region of the 5′ NCR can interact to lesser extents. Finally, we show that both of these RNA-protein interactions are conserved among the closely related enteroviruses PV1 and coxsackievirus type B3, human rhinovirus type 14, and the more distantly related cardiovirus Theiler's murine encephalomyelitis virus, suggesting that such RNA-protein interactions serve basic functions which are conserved and utilized by each of these picornaviruses.

Components required for the cap-independent internal initiation of picornavirus RNAs are clearly present in the uninfected cell since picornavirus RNAs are initially translated in the cell in the absence of other viral gene products. In addition, these RNAs can be translated in vitro in extracts or lysates made from uninfected cells. Poliovirus (PV) mRNAs are relatively poor mRNAs in comparison with most cellular mRNAs in some in vitro systems (7, 24), but upon the addition of HeLa cell extracts, the translation of wild-type PV RNA can be greatly stimulated (2, 7). As we have shown previously, certain mutations in the 5′ noncoding region (5′ NCR) reduce or negate the ability to respond to these translation stimulatory factors (6). Presumably, the stimulatory effect is due to a direct interaction between proteins in these extracts and the sequences or structures in the 5′ NCR required for cap-independent translation. Therefore, 5′ NCR mutants which are not able to respond to the stimulatory factors either must be unable to directly interact with these factors, or the interaction may not be a functional one.

Employing mobility shift electrophoresis assays and UV cross-linking experiments, a number of groups have recently shown specific interactions between cellular proteins and RNA structures or sequences in the PV 5′ NCR as well as the 5′ NCRs of encephalomyocarditis virus RNA and foot-and-mouth disease virus RNA (1, 4, 13, 19, 20, 22). The regions in the PV 5′ NCR that were involved in RNA-protein interactions included nucleotides 178 to 224 (22), 97 to 182 and 510 to 629 (4), and 559 to 624 (20). The nucleotide 178 to 224 RNA-protein complexes were shown by UV cross-linking to involve a 50-kDa cellular protein that may be membrane associated (22). The RNA-protein complexes which formed between nucleotide 97 to 182 and 510 to 569 RNAs were composed of a number of distinct cellular proteins that included eukaryotic initiation factor 2α (4). Finally, the RNA-protein complex specific for the nucleotide 559 to 624 region of the PV 5′ NCR was shown to contain a cellular polypeptide of 52 kDa that was not a known initiation factor (20), and a recent report has shown that there may be an additional binding site for this protein in the 5′ NCR of mutant viral genomes (9). The functional significance of such interactions remains to be elucidated, but perhaps they involve novel cellular factors utilized in the initiation of cap-independent translation of viral messages as well as cellular messages since these proteins are present in extracts from uninfected cells.

The RNA-protein interaction between an in vitro-synthesized RNA from nucleotides 178 to 224 and a 50-kDa cellular protein described by Najita and Sarnow (22) was of particular interest, since our previous work had identified a number of biologically important mutations within and proximal to this region of the PV 5′ NCR. This RNA sequence corresponds to stem-loop D (refer to Fig. 1 for the predicted RNA secondary structure of the PV type 1 [PV1] 5′ NCR). Previous results from our laboratory have shown that se-

* Corresponding author.

quences 184 to 228 (inclusive of stem-loop D) are not required for a productive viral infection since these sequences were found to be deleted in the revertant virus, R2 (5). The R2 revertant virus relieved the temperature-sensitive (*ts*) phenotype of a four-nucleotide deletion of 221 to 224 found in the 220D1 mutant virus. In addition, this structure is also deleted in the nucleotide sequence of bovine enterovirus (8). If stem-loop D does not appear to be absolutely required for virus growth in tissue culture, then, in turn, the stem-loop D RNA-protein interaction may not be absolutely required either. Although the R2 revertant relieves the *ts* defect of the 220D1 mutant, it is not a completely wild-type virus as it exhibits slower growth at both 33 and 37°C when compared with wild-type PV1 (5). When translated in vitro, RNAs containing the R2 deletion are not as efficient as wild-type RNAs (6), suggesting that these sequences in fact contribute to the full translational potential of the 5′ NCR. Najita and Sarnow (22) have also reported that the presence of the 50-kDa protein in extracts is dependent on Nonidet P-40 (NP-40) lysis of cells. Their results suggested that this protein is membrane associated and that the stem-loop D RNA-protein interaction augments viral functions which require membranes.

We have described the detrimental effects on translation of a number of mutations which alter the spacing between two predicted stem-loop structures in the PV1 5′ NCR (6). These two structures are stem-loop D (nucleotides 186 to 220) and stem-loop E (nucleotides 234 to 440). The RNA mobility shift assay was used in the present study to further define the effects of mutations which have altered spacing in the 5′ NCR of PV RNA as well as some additional mutations constructed to specifically define the RNA substrate requirements for these interactions. Specifically, RNAs containing mutations near and within stem-loop D were analyzed for their ability to bind cellular factors from uninfected HeLa extracts. We found that RNA containing the 220D mutation, which resulted in a virus with *ts* defects, showed no defect in the ability to interact with the stem-loop D binding protein(s). Using site-directed mutations, we show that maintenance of the structure of stem-loop D is essential for the RNA-protein interaction. In addition, this RNA-protein interaction is conserved among the 5′ NCRs of coxsackievirus B3 (CVB3), human rhinovirus 14 (HRV14), and Theiler's murine encephalomyelitis virus (TMEV), and the RNA binding activity is present in HeLa, NGP (a neuroblastoma cell line), and BHK-21 (baby hamster kidney) cells as well as in rabbit reticulocyte lysate (RRL).

According to the computer-predicted models for the secondary structure of the 5′ NCR of PV, stem-loop E encompasses nucleotides 234 to 440 and contains a number of smaller stem-loop structures within it (12, 27, 28, 32). This region is well within the area defined as essential for cap-independent translation and internal ribosome binding in PV RNA (25, 26, 34, 35). The structure of stem-loop E is conserved among PV strains and also among CVB3, HRV2, and HRV14 (28). Although an RNA-protein interaction occurring in this region has not been described, a number of mutations and their effects on viral functions have been previously described. Infectivity and virus growth experiments with the recombinant virus PCV305 showed that CVB3 sequences can substitute for PV1 sequences in the nucleotide 1 to 627 region of viral RNA and provide the necessary wild-type functions to the virus, suggesting that the conservation of RNA secondary structure is more important than the actual nucleotide sequences (14). Trono et al. (34) constructed a number of small insertions within the nucleotide 234 to 440 region which produced mutant viruses with *ts*, small-plaque, or wild-type phenotypes or were lethal to virus production. These results show that small insertions in the predicted stem-loop E structure can have drastic effects on viral functions, suggesting that the region which is perturbed plays an important role.

The existence of a protein interaction with sequences or structures in stem-loop E of the PV1 5′ NCR was investigated in the present study. Using the RNA mobility shift assay, we found that a cellular protein present in the A cut (0 to 40% ammonium sulfate cut) of a ribosomal salt wash (RSW) from HeLa cells forms a complex with stem-loop E RNA. Using smaller RNAs as unlabeled competitors, the sequences necessary for this interaction have been narrowed down to approximately nucleotides 260 to 415, which encompass the outer stem-loop structures present within stem-loop E. This RNA-protein interaction is conserved among PV1, CVB3, and HRV14 as well as the more distantly related cardiovirus TMEV. The RNA binding activity is present in extracts from HeLa, NGP, and BHK-21 cells as well as in RRL, suggesting that this protein(s) plays an important role in the life cycles (and perhaps the cap-independent translation) of each of these picornaviruses.

MATERIALS AND METHODS

Construction of transcription templates. (i) pT747. The vector pT747 was constructed from pT7-P3μ2 (36), which has a *Pst*I linker inserted at the *Hgi*AI site at nucleotide 747. pT7-P3μ2 contains the pGEM-1 transcription vector background and utilizes a *Pst*I site in the polylinker to linearize just downstream of the inserted PV1 sequences. pT7-P3μ2 was digested with *Pst*I, the ~3.6-kbp fragment containing the pGEM-1 vector sequences plus the PV1 5′ NCR from nucleotides 1 to 747 was gel purified and incubated with T4 DNA ligase, and competent C600 cells were transformed. In all cases, transformants were screened by restriction enzyme digestion, and ultimately $CsCl_2$-pure DNA was sequenced (33, 37). This yielded a transcription vector with a 5′ end similar to pT7-1, the PV1 5′ NCR including the first AUG and the second codon of the polyprotein, and then unique *Pst*I and *Hin*dIII restriction enzyme sites.

(ii) pT629. The pT747 construct described above was digested with *Msc*I, which cuts at nucleotide 627, and *Pst*I, which cuts in the polylinker sequence directly 3′ to the inserted PV1 sequences. The digested DNA was then treated with mung bean nuclease (New England BioLabs), incubated with T4 DNA ligase, and transformed into competent C600 cells. This yielded a vector similar to pT747 except that it contained only PV1 sequences from nucleotides 1 to 629 and then a unique *Hin*dIII site. The pTΔE construct was created by digesting the pT629 vector with *Bam*HI and *Bsm*I, which cut in the PV sequences at nucleotides 220 and 456, respectively, and then by incubating with the Klenow enzyme to produce blunt ends. The ~3.2-kbp band containing the pGEM-1 vector sequences plus PV sequences 1 to 224 and 463 to 629 was isolated and incubated with T4 DNA ligase, and competent cells were transformed.

(iii) pT-N183μ, pT-LSD, and pT-LSR. A unique *Sma*I or *Ava*I site was created just upstream from the base of stem-loop D in the pT629 vector by single-stranded oligonucleotide mutagenesis (11). An oligonucleotide was synthesized (Operon Technologies) corresponding to PV1 sequences 175 to 194 of minus-strand polarity. The oligonucleotide contained a single nucleotide change at 183 from the wild-type T to a G, creating a unique *Sma*I or *Ava*I

restriction enzyme site. The presence of a unique restriction site on the 5′ side (*Sma*I or *Ava*I) and the 3′ side (*Bam*HI) of stem-loop D in pT-N183μ allowed for the construction of additional stem-loop D mutants by double-stranded oligonucleotide cassette mutagenesis. pT-LSD, the lower stem-loop D disruption mutation, was constructed by using two double-stranded oligonucleotide cassettes. Oligonucleotides SD13 and SD14 correspond to wild-type sequences for 179 to 199 for the positive strand and 183 to 199 for the minus strand, respectively. Oligonucleotides SD15 and SD16 correspond to sequences from 200 to 220 for the positive strand and 200 to 224 for the minus strand, respectively, and, in addition, contained nucleotide sequence substitutions at 215 to 220 from the wild-type CGACG to TCTAC. These nucleotide substitutions generate a unique *Acc*I site. The SD13 and SD14 and SD15 and SD16 oligonucleotides were annealed, incubated with T4 polynucleotide kinase (U.S. Biochemical Corp.) and ATP, and ligated to a gel-purified *Ava*I-to-*Bam*HI fragment from pT-N183μ. Transformants were initially screened for the presence of the new *Acc*I site. pT-LSR, the lower stem-loop D restoration mutant, was constructed by double-stranded oligonucleotide mutagenesis utilizing the SD15 and SD16 oligonucleotides described above along with two new oligonucleotides, SD17 and SD18. SD17 and SD18 correspond to PV1 sequences from 179 to 199 for the positive strand and 183 to 199 for the minus strand, respectively, and, in addition, contain nucleotide sequence substitutions at 186 to 190 from the wild-type TGCTG to GTAGA. Oligonucleotides were annealed and ligated, and transformants were screened as described above for the pT-LSD mutant.

(iv) pT220-460. The plasmid pT220-460 was constructed from pT7-P1-K-Δ1-220 which contained a deletion of nucleotides 1 to 220 in the pT7-P1-K vector described previously (6). This vector was digested with *Bsm*I, which cuts at nucleotide 456, and *Pst*I, which cuts in the polylinker sequence. The fragments were treated with mung bean nuclease to delete the overhanging nucleotides from the *Bsm*I and *Pst*I sites. The resulting ~3,050-bp *Bsm*I-*Pst*I fragment was gel purified and incubated with T4 DNA ligase, and competent C600 cells were transformed. pT220-460 linearized at (i) *Hin*dIII in the polylinker 3′ to the insert was the template for the 220 to 460 RNA, (ii) *Nco*I (nucleotide 392) was the template for the 220 to 392 RNA, and (iii) *Ear*I (nucleotide 415) was the template for the 220 to 415 RNA. Each of these RNAs contained pGEM-1-derived vector sequences GGGAGACCG 5′ to the PV1 sequences, while the 220 to 460 RNA also contained pGEM-1-derived vector sequences GUUCGA 3′ to the PV1 sequences.

(v) pT274-415. The pT220-460 vector described above was digested with *Ear*I, which cuts in the pT220-460 PV sequences at nucleotide 415 and the pGEM-1 vector sequences at nucleotides 152 and 1956. An ~250-bp *Ear*I-*Ear*I fragment encoding PV1 sequences 220 to 415 and pGEM-1 vector sequences ~50 to 152 was purified by agarose gel electrophoresis. The 250-bp fragment was then digested with *Taq*I, which cuts at 246 and 274 in the PV sequences of the fragment. The ~140-bp *Taq*I-*Ear*I fragment containing PV sequences from 274 to 415 was made blunt by filling in the overhanging ends with the Klenow fragment of DNA polymerase I. The 140-bp fragment and a pGEM-1 vector fragment (which had been digested with *Eco*RI and *Pst*I in the polylinker and treated with mung bean nuclease to delete the overhanging nucleotides) were incubated with T4 DNA ligase. Competent C600 cells were transformed and screened by restriction enzyme digestion to verify the correct size of the insert. pT274-415 linearized at (i) the *Hin*dIII site in the polylinker 3′ to the insert was the template for the 274 to 415 RNA, and (ii) *Rma*I (nucleotide 400) was the template for the 274 to 400 RNA. Each of these RNAs contained pGEM-1-derived vector sequences GGGAGACCGG 5′ to the PV1 sequences and the 274 to 415 RNA also contained the sequence AGCCAAGCU 3′ to the PV1 sequences.

(vi) pT274-392. The pT747 vector described above was digested with *Taq*I and *Nco*I and then treated with the Klenow enzyme to fill in the overhanging ends. The 118-bp fragment containing PV sequences from 274 to 392 was gel purified and incubated with the pGEM-1 vector fragment described above for the pT274-415 vector and T4 DNA ligase before transformation. pT274-392 linearized at the *Hin*dIII site in the polylinker 3′ to the insert was the template for the 274 to 392 RNA. The 274 to 392 RNA contained pGEM-1-derived sequences GGGAGACCGG and AGCCCAAGCU 5′ and 3′, respectively, to the PV1 sequences.

(vii) pT311-415. pT274-415 was digested with *Pvu*II and *Hin*dIII. *Pvu*II cuts at nucleotide 98 in the pGEM vector sequences on the 5′ side of the insert, and *Hin*dIII cuts in the polylinker on the 3′ side of the insert. The ~190-bp *Pvu*II-*Hin*dIII fragment was isolated and then digested with *Alu*I, which cuts at nucleotide 310 in the PV1 sequences. The resulting 110-bp *Alu*I-*Hin*dIII fragment was incubated with T4 DNA ligase and a pGEM-1 vector fragment which had been digested with *Eco*RI, treated with mung bean nuclease to blunt the *Eco*RI site, and then digested with *Hin*dIII. pT311-415 linearized at the *Hin*dIII site in the polylinker 3′ to the insert was the template for the 311 to 415 RNA. The 311 to 415 RNA contained pGEM-1-derived vector sequences GGGAGACCGG and AGCCCAAGCT 5′ and 3′, respectively, to the PV1 sequences.

(viii) pT311-400. pT629 was digested with *Bam*HI and *Bsm*I, and the resulting 240-bp fragment encoding PV sequences 220 to 460 was gel purified. The 240-bp fragment was then digested with *Rsa*I, *Alu*I, and *Rma*I, which cut at 256, 310 and 430, and 400, respectively. The 90-bp *Alu*I-*Rma*I fragment encoding PV sequences 311 to 400 was gel purified, treated with Klenow enzyme to fill in the overhanging ends, and then ligated to the pGEM-1 vector fragment described above for the pT274-415 plasmid. pT311-400 linearized at the *Hin*dIII site in the polylinker 3′ to the insert was the template for synthesis of the 311 to 400 RNA. The 311 to 400 RNA contained pGEM-1-derived vector sequences GGGAGACCGG and CCCAAGCT 5′ and 3′, respectively, of the PV1 sequences.

In vitro transcription. Before transcription, all plasmid DNAs were linearized by complete digestion with the appropriate restriction enzyme. pT747 and pT629 DNA constructs, linearized with *Hin*dIII, were the templates for transcription of the 1 to 747 and 1 to 629 RNAs, respectively. pT747 DNA constructs, linearized with *Taq*I, were the template for transcription of the 1 to 246 RNAs. The pT7-CVB3-5′ construct (18) containing CVB3 sequences 1 to 750, linearized with *Taq*I and *Ava*I, was the template for transcription of the CVB3 1 to 250 and 1 to 750 RNAs, respectively. The pT7-HRV14 construct containing a full-length cDNA copy of the HRV14 genome (21) in the pGEM-1 transcription vector background linearized with *Sna*BI and *Bcl*I was the template for transcription of the HRV14 1 to 260 and 1 to 628 RNAs, respectively (22a). The TMEV subgenomic cDNA was a derivative of a full-length cDNA copy of the TMEV genome in a T7 promoter-based background (30). Linearization at the Asp-718 site in the 5′ NCR produced the template for the TMEV 1 to 930 RNA.

Conditions for in vitro transcription were the same as described previously (6) except that transcription reactions were treated with 30 U of DNase I (Worthington Biochemicals) for 10 min at 37°C to degrade the DNA template (~3 μg). Unlabeled RNAs were ethanol precipitated twice and quantitated by reading the A_{260}. All RNAs (^{32}P-labeled and unlabeled) were analyzed for correct size by running equivalent amounts on denaturing 7 M urea–acrylamide gels and visualizing by ethidium bromide staining and/or exposure to XAR (Kodak) film.

Preparation of cell extracts. Preparation of HeLa S10, RSW, and ammonium sulfate cuts was as described previously (2, 7, 10). Preparation of S10 extract from BHK-21 cells was essentially as described for HeLa cells. NP-40 lysis of HeLa cells was essentially as described previously (22, 31). The human neuroblastoma cell line, NGP, was a generous gift from Eric Stanbridge, University of California, Irvine, and was adapted to grow in suspension culture (22a). NP-40 lysis of neuroblastoma cells (NGP) and preparation of extract was the same as for HeLa cells. RRL was obtained from Promega Biotec.

RNA mobility shift assay. The RNA mobility shift assay was done essentially as described originally by Konarska and Sharp (17) with only minor modifications. Briefly, the protein extract was preincubated with either 4 μg of poly(dI-dC) (Sigma) or 5 to 11 μg of tRNA (Sigma) in binding buffer (25 mM KCl, 5 mM HEPES [*N*-2-hydroxyethylpiperazine-*N'*-2-ethanesulfonic acid] [pH 7.5], 2 mM $MgCl_2$, 0.1 mM EDTA, 3.8% glycerol, 2 mM dithiothreitol) in a final volume of 10 μl for 10 min at 30°C. For competition experiments, unlabeled RNAs were lyophilized in the tube and included in the preincubation step. An aliquot (0.5 pmol) of ^{32}P-labeled RNA was added, and the incubation was continued for 10 min. Heparin was then added to 0.5 or 5.0 mg/ml, and the mixture was incubated for an additional 10 min at 30°C. Glycerol was then added to a final concentration of 10%, and the samples were loaded on a 4% polyacrylamide (40:1 acrylamide-bisacrylamide)–5% glycerol–0.5× TBE (45 mM Tris-borate, 1 mM EDTA) gel. The gel had been prerun for approximately 30 min at 200 V. Samples were electrophoresed at 4°C at constant voltage until the xylene cyanol in a marker lane had run 10 to 12 cm from the top of the gel. The gels were fixed in 5% methanol–10% acetic acid, dried, and exposed to XAR film.

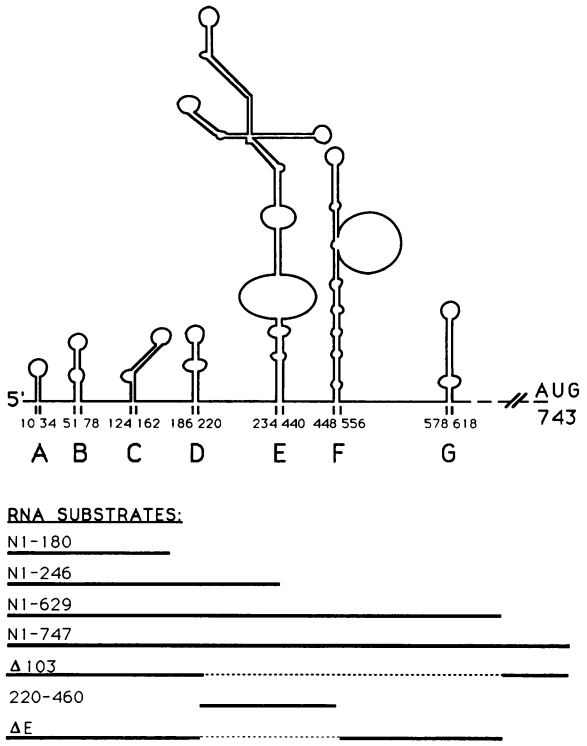

FIG. 1. RNA substrates utilized in the mobility shift assays. A linear diagram of the computer-predicted RNA secondary structure of the PV1 5′ NCR is shown at the top of the figure. This figure is based on the predictions of Pilipenko et al. (27) with modifications by Jackson et al. (12). The stem-loop structures are lettered from A to G. Below the structure the RNA substrates used in the mobility shift assays are shown. RNAs were synthesized in vitro by T7 RNA polymerase as described in Materials and Methods. N, nucleotide.

RESULTS

PV RNA containing sequences 1 to 246 interacts with proteins in different extracts of HeLa cells. We investigated the RNA-protein interaction between PV1 sequences in stem-loop D and the cellular 50-kDa protein described by Najita and Sarnow (22). The computer-predicted RNA secondary-structure model of the PV1 5′ NCR is illustrated in Fig. 1 (12, 27, 28, 32). The boundaries of the predicted stem-loop structures are indicated by the nucleotides which form the base of each stem-loop structure and which are given letter designations. Some of the RNA substrates utilized in the experiments described in this report are illustrated below the structure shown in Fig. 1. An RNA containing nucleotide sequences 1 to 246 was used as the ^{32}P-labeled substrate in the experiments investigating the stem-loop D RNA-protein interaction. The data in Fig. 2A show that the 1 to 246 RNA binding activity was present primarily in the supernatant of NP-40-lysed HeLa cells which were fractionated by ammonium sulfate precipitation to a 0 to 60% ammonium sulfate cut and the 60%+ supernatant (Fig. 2A, compare lanes 2 to 6 with lanes 7 to 9). Our experiments show that the decreased mobility of the RNA is due to formation of an RNA-protein complex since proteinase K treatment of the extract either before addition to the binding reaction (lane 12) or after the binding reaction (lane 13) returned the RNA to its free (F) form. The data shown in Fig. 2B show that a 1 to 246 RNA binding activity was also found in HeLa cell extracts which are enriched in translation initiation factors and that NP-40 lysis of the HeLa cells is not necessary to obtain this activity. The RNA binding activity was found in S10 extracts (lanes 3 to 5), RSW (lanes 6 to 8), and the RSW 40 to 70% ammonium sulfate or B cut (lanes 12 to 14), but not in the RSW 0 to 40% ammonium sulfate or A cut (lanes 9 to 11). Note that the very slowly migrating and smeared complexes in these reactions are most likely due to nonspecific interactions since heparin was not added to these reactions.

Competition experiments for the stem-loop D RNA-protein interaction. Previous genetic and biochemical analysis of a number of mutant PV RNAs suggested that the maintenance of the proper spacing between stem-loops D and E in the PV1 5′ NCR was necessary for wild-type viral growth properties and wild-type levels of translation in vitro (5, 6). We wanted to investigate whether any of the mutations near stem-loop D had an effect on the stem-loop D RNA-protein interaction. Competition experiments with unlabeled (cold) competitor RNAs are shown in Fig. 3. The mobility shift from free 1 to 246 RNA (F) to complexed RNA (C) upon the

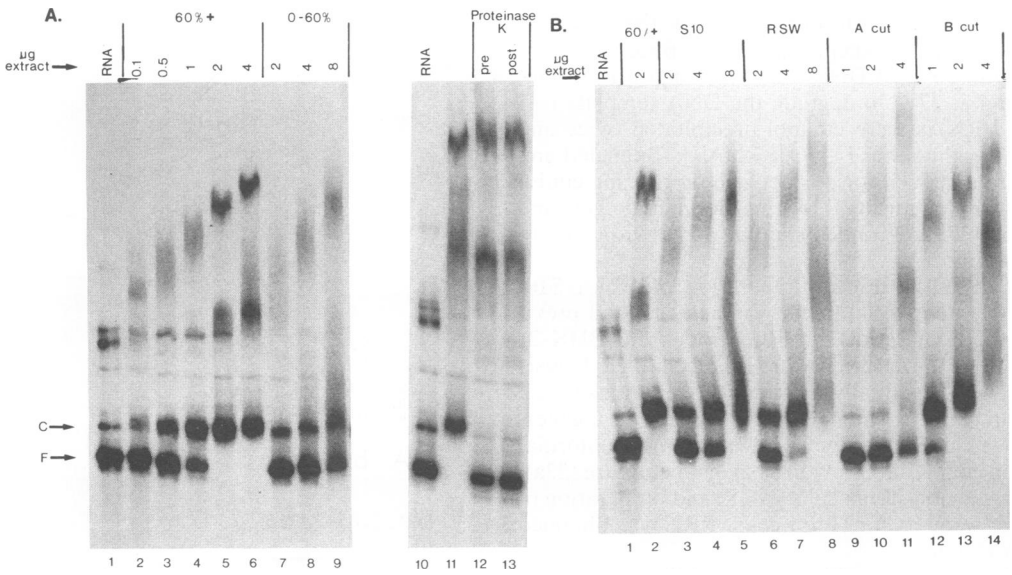

FIG. 2. PV1 1 to 246 RNA interacts with a cellular protein from different extracts of HeLa cells. ^{32}P-labeled 1 to 246 RNA was tested in binding reactions for formation of complexes with protein(s) in extracts from NP-40-lysed HeLa cells (A) and S10 and RSW extracts from HeLa cells (B). (A) Lanes 1 and 10 contain RNA alone in buffer with the predominant free form marked by the F. Lanes 2 to 6 contain an increasing amount (from 0.1 to 4.0 µg) of the 60%+ extract, and lanes 7 to 9 contain an increasing amount of the 0 to 60% extract (2 to 8 µg). Lane 11 contains 2 µg of the 60%+ extract. (B) Lanes 1 and 2 show the mobility shift from free 1 to 246 RNA (F) to complexed RNA (C) upon the addition of 4 µg of the 60%+ extract. The remaining lanes contain an increasing amount of the following extracts: 2, 4, and 8 µg of HeLa S10 (lanes 3 to 5); 2, 4, and 8 µg of an RSW (lanes 6 to 8); 1, 2, and 4 µg of an RSW A cut (lanes 9 to 11); and 1, 2, and 4 µg of an RSW B cut (lanes 12 to 14). Binding reactions were performed as described in Materials and Methods except that there was no heparin treatment of these reactions. A 0.5-pmol sample of ^{32}P-labeled RNA was used in each reaction. Proteinase K treatment consisted of 25 µg of proteinase K added to the preincubation step (lane 12) or added after the binding reaction (lane 13) and incubated for an additional 10 min at 30°C.

addition of extract is shown in lanes 1 and 2. We observed competition for complex formation upon the addition of 2- and 10-fold molar excesses of the unlabeled wild-type 1 to 246 RNA (refer to lanes 3 and 4). In addition, competition for complex formation can occur in the context of the entire PV1 5′ NCR (1 to 747) as shown by the data presented in lanes 5 and 6. An RNA from 1 to 747 missing 184 to 228 (R2; Fig. 3, lanes 7 and 8) could not compete for complex formation, whereas RNAs from 1 to 747 containing deletions of 221 to 224 (220D, lanes 9 and 10) or 461 and 462 (456D2, lanes 11 and 12) could compete for complex formation. An RNA from 1 to 180 (lanes 13 and 14) was also unable to compete for complex formation. The results from the competition experiments utilizing a 1 to 747 RNA containing the R2 deletion and the 1 to 180 RNA show that the mobility shift observed for the 1 to 246 RNA is due to an interaction of the protein(s) with the RNA sequences in stem-loop D as expected. The two mutations, 220D and 456D2, despite resulting in a *ts* virus and being lethal to virus production, respectively, do not affect the ability of stem-loop D within their respective 5′ NCR RNAs to interact with the protein(s) in this extract. In addition, comparison of results from RNA binding-competition experiments performed at 30 and 37°C revealed no *ts* defect in the ability of an RNA containing the 220D mutation to compete for stem-loop D binding (data not shown). These data suggest two possibilities: (i) the inability to form the stem-loop D RNA-protein interaction is not the cause of the in vivo phenotypes observed for these mutations; and (ii) if the intact structure of stem-loop D is necessary for a specific RNA-protein interaction, then neither of these mutations (220D or 456D2) has a global effect on the RNA secondary structure which affects stem-loop D.

Disruption of the lower stem structure of stem-loop D. The predicted base-paired structure in the lower stem of stem-loop D occurs with varying thermodynamic stabilities among the PV serotypes and HRV14, and the lower stem may not exist in CVB3 (Fig. 4). In addition, there appears to be very little conservation of the nucleotide sequence in the lower stem among these different picornaviruses. To determine whether the maintenance of the lower stem structure is required for the RNA-protein interaction between the PV1 stem-loop D and the protein(s) in the 60%+ extract, we constructed a mutation in the PV1 5′ NCR by double-stranded oligonucleotide cassette mutagenesis (described in Materials and Methods) designed to disrupt the formation of the lower stem of stem-loop D. The sequence change of the lower stem disruption (LSD) mutant is shown in Fig. 5A. Nucleotides 216 to 220 were replaced with an *Acc*I restriction site sequence which would virtually abolish all potential base pairing with 186 to 190 as shown in Fig. 5A. The results from RNA mobility shift assays with the LSD mutant as an unlabeled competitor against the wild-type 1 to 246 RNA are shown in Fig. 5B. An approximately 10-fold molar excess of wild-type RNA was able to compete for all binding in this assay, but even as much as a 40-fold molar excess of the LSD mutant RNA was not able to compete at all for complex formation. Note that a 20-fold molar excess of wild-type RNA from 1 to 629 was able to compete for all binding, whereas a 1 to 629 RNA containing the LSD mutation was not (lanes 12 and 13). In addition, ^{32}P-LSD 1 to 246 RNA also could not form an RNA-protein complex when tested directly in the RNA mobility shift assay (data not shown).

The above results suggested either that maintenance of the base-pairing potential of the lower stem of PV1 was essential

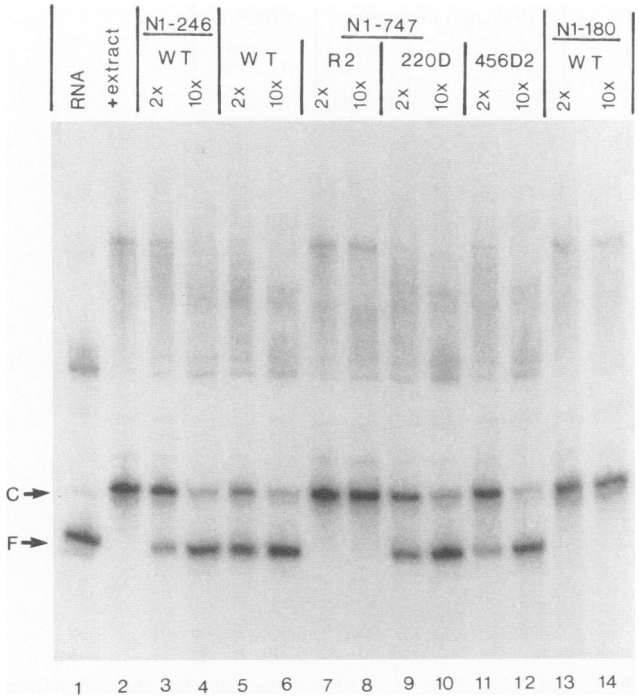

FIG. 3. 5′ NCR mutant RNAs compete for the stem-loop D RNA-protein interaction. Binding reactions were performed as described in Materials and Methods with heparin treatment at 0.5 mg/ml. Lanes 1 and 2 show the mobility shift from free 1 to 246 RNA (F) to complexed RNA (C) upon the addition of 4 μg of 60%+ extract. Reactions in lanes 3 to 14 contain 4 μg of the 60%+ extract and the indicated molar excess (2× or 10×) of unlabeled (cold) competitor RNAs in the preincubation step to which 0.5 pmol of ^{32}P-labeled 1 to 246 RNA was added. WT indicates wild-type 5′ NCR RNA sequences (lanes 3 to 6). R2 contains a deletion of 184 to 228 (lanes 7 and 8). 220D contains a deletion of 221 to 224 (lanes 9 and 10). 456D2 contains a deletion of 461 and 462 (lanes 11 and 12). The size of the unlabeled (cold) RNA is indicated above the lanes (N1-246, N1-747, or N1-180).

for an RNA-protein interaction or that specific sequences in this region were essential and that these sequences had been altered in the LSD mutation. To test these two possibilities, we constructed an additional mutation which restored the base-pairing potential to the lower stem of stem-loop D. The

U G		C	C A	C C	C C	C A	C C
U C							A
N200 CG N205		UA		UA	UA		UA
GU		GC	GC	GC	GC	GC	GC
UG							U U
CG							
AU		GC					GC
A GU G A U A A UG A			A CG	CG	CG	A G G	GC A
GC			GU	GU	GU	C A	
CG	UG	UG	UG			UG	GC
UA		CG		CG	C U	A A	AU
GC			AU			UA	GU
N186 UG N220		GU	C C	GC	GC	G A	C U
PV1	PV1S	PV2	PV2S	PV3	PV3S	CVB3	HRV14

FIG. 4. Nucleotide sequence conservation in stem-loop D between PV strains and CVB3 and HRV14. The complete nucleotide sequence of stem-loop D for PV1 is listed, and only the single nucleotide or base-pair differences are listed for the other viral sequences. Blank spaces indicate that the same nucleotide is present as in PV1.

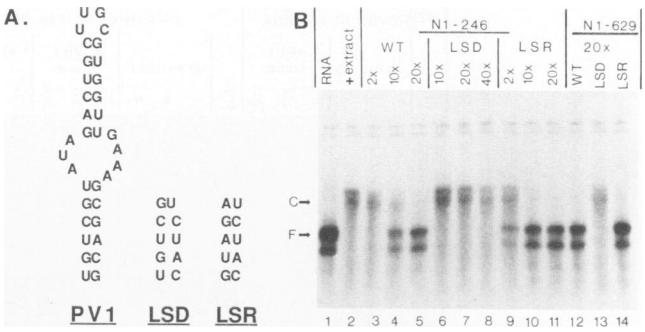

FIG. 5. Importance of base-pairing potential in the lower stem of stem-loop D. (A) Nucleotide sequence of stem-loop D and nucleotide changes to the lower stem in the LSD and LSR mutants. (B) Results of competition experiments with unlabeled competitor RNAs encoding the LSD and LSR mutants. All lanes contain 0.5 pmol of ^{32}P-labeled 1 to 246 RNA, and lanes 2 to 14 contain 4 μg of the 60%+ extract. All reactions were treated with heparin at 0.5 mg/ml. Lanes 1 and 2 show the mobility shift observed from free RNA (F) to complexed RNA (C) upon the addition of 4 μg of the 60%+ extract. Lanes 3 to 5 contain the indicated molar excess of unlabeled wild-type 1 to 246 RNA, lanes 6 to 8 contain the indicated molar excess of unlabeled 1 to 246 RNA containing the LSD mutation, and lanes 9 to 11 contain the indicated molar excess of unlabeled 1 to 246 RNA containing the LSR mutation. Reactions in lanes 12 to 14 contained a 20-fold molar excess of unlabeled 1 to 629 RNAs encoding wild-type, LSD, or LSR sequences, respectively, in the preincubation step.

nucleotide sequence of the stem-loop restoration (LSR) mutant is illustrated in Fig. 5A. The LSR mutant contains the original LSD mutation as well as nucleotide changes from 186 to 191 on the opposite side of the lower stem structure. The LSR mutant encodes sequences in the lower stem that, if base paired, would have thermodynamic stability similar to that of the wild-type lower stem structure but nucleotide sequences very different from those of the wild type on both strands of the stem structure. The results from RNA mobility shift assays with the LSR mutant as an unlabeled competitor against the wild-type 1 to 246 RNA are shown in Fig. 5B. Similar to a wild-type competitor (lanes 3 to 5), RNA containing the LSR mutation was able to compete fully for the interaction between stem-loop D and a protein(s) in the 60%+ extract (refer to lanes 9 to 11). A 1 to 629 RNA containing the LSR mutations was also able to compete for binding as well as the wild-type 1 to 629 RNA (compare lane 14 with lane 12). In addition, a ^{32}P-LSR 1 to 246 RNA was able to form a specific RNA-protein complex when tested directly in the RNA mobility shift assay (data not shown).

The above results suggest that maintenance of the lower stem structure in stem-loop D is essential for the RNA-protein interaction observed for PV1 RNA and that the nucleotide sequence changes made in the original LSD mutant are not themselves detrimental to this RNA-protein interaction since these nucleotide sequence changes are also present in the LSR mutant, which is able to interact with the protein(s) in the 60%+ extract. In addition, the nucleotide sequence substitutions in both strands of the lower stem structure in the LSR mutation must not change any requirements for a direct RNA-protein interaction with the lower stem (if indeed such an interaction occurs).

Conservation of stem-loop D RNA-protein interactions among picornaviruses. A high degree of nucleotide sequence conservation exists among different picornaviruses. For

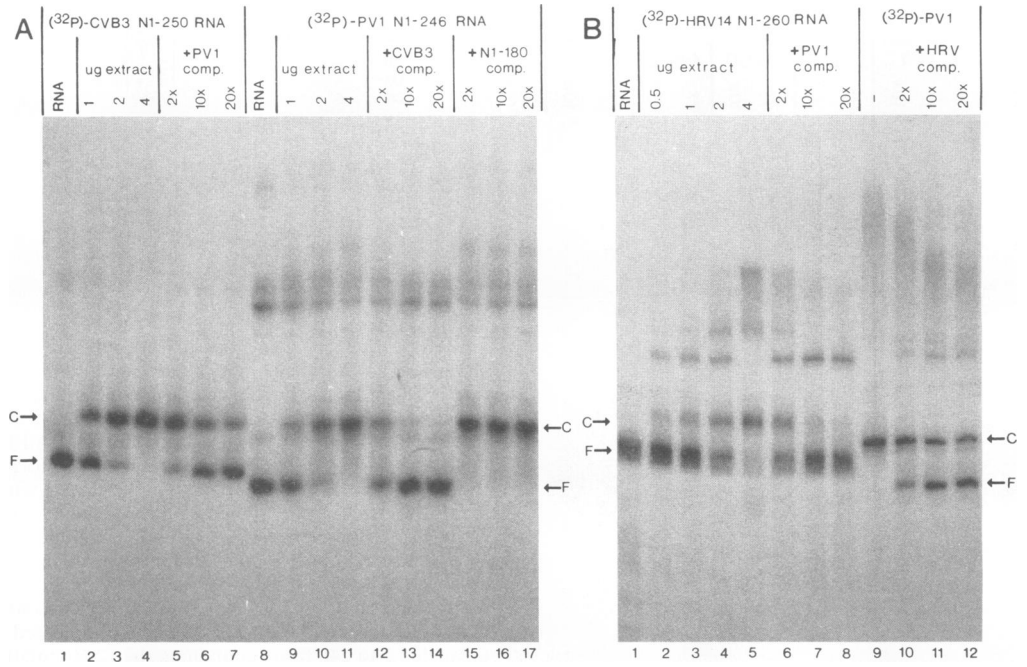

FIG. 6. Conservation of stem-loop D RNA-protein interaction among PV1, CVB3, and HRV14. (A) RNA mobility shift and competition experiments with CVB3 RNA substrates; (B) with HRV14 RNA substrates. All reactions were performed as described in Materials and Methods, contained 0.5 pmol of ^{32}P-labeled RNA, and were treated with 0.5 mg of heparin per ml. (A) Lanes 1 to 7 contain ^{32}P-CVB3 1 to 250 RNA either alone (lane 1) or in the presence of 1, 2, or 4 μg of the 60%+ extract (lanes 2 to 4, respectively). Reactions in lanes 5 to 7 contain 4 μg of the 60%+ extract and the indicated molar excess of unlabeled PV1 1 to 246 RNA in the preincubation step. Lanes 8 to 17 contain ^{32}P-PV1 1 to 246 RNA. The reaction in lane 8 contains RNA alone, while lanes 9 to 11 contain 1, 2, and 4 μg, respectively of the 60%+ extract. Reactions in lanes 12 to 14 contain 4 μg of the 60%+ extract and the indicated molar excess of unlabeled CVB3 1 to 250 RNA. Reactions in lanes 15 to 17 contain 4 μg of the 60%+ extract and the indicated molar excess of unlabeled PV1 1 to 180 RNA in the preincubation step. (B) Lanes 1 to 8 contain 0.5 pmol of ^{32}P-HRV14 1 to 260 RNA. Lanes 1 to 5 display the mobility shift observed for the ^{32}P-HRV14 1 to 260 RNA from the free form (F, lane 1) to the complexed form (C) upon the addition of an increasing amount (0.5, 1, 2, and 4 μg) of the 60%+ extract. Reactions in lanes 6 to 8 contain 4 μg of the 60%+ extract and the indicated molar excess of unlabeled PV1 1 to 246 RNA. Reactions in lanes 9 to 12 contain ^{32}P-PV1 1 to 246 RNA, 4 μg of the 60%+ extract, and the indicated molar excess of unlabeled HRV14 1 to 260 RNA.

instance, in the 5′ NCRs of PV1 and CVB3 there is 70% sequence conservation, and there is 65% conservation between PV1 and HRV14. Computer-predicted models of the secondary structure of these picornaviruses suggest that the conservation of RNA secondary structure is even higher (12, 27, 28, 32). Apparently, this conservation extends to the functions of these regions as well. It was shown that the recombinant virus PCV305, containing the 5′ NCR of CVB3 and the coding region of PV1, had essentially wild-type PV1 growth properties (14). If the RNA-protein interaction with stem-loop D provides a necessary function to PV1, a functionally equivalent interaction must also occur with CVB3 since the nucleotide sequence of stem-loop D in the PCV305 recombinant is derived from CVB3. Stem-loop D appears to be present in the 5′ NCRs of the genomes of these picornaviruses (PV1, CVB3, and HRV14), although the entire structure may not be completely conserved. Figure 4 displays the nucleotide sequences of the poliovirus serotypes, CVB3, and HRV14 within stem-loop D. Initial observation reveals a high degree of sequence conservation in the upper stem, loop, and bulge sequences, while the lower stem contains little sequence conservation and displays variable degrees of predicted thermodynamic stability. Our results showed that maintenance of the base-pairing potential of the lower stem of PV1 stem-loop D was essential for the RNA-protein interaction (Fig. 5). Since the lower stem does not appear to be present in CVB3, it was important to determine whether the RNA-protein interaction was conserved between PV1 and CVB3 since there is functional conservation between the 5′ NCRs of these two viruses. Recombinant constructs have not been made between HRV14 and PV1, but due to the sequence and structural conservation, it was of interest to determine whether there was conservation of the stem-loop D RNA-protein interaction among HRVs and PVs.

The mobility shift assays and competition experiments with CVB3 RNA sequences are shown in Fig. 6A. When an increasing amount of 60%+ extract was added to the binding reactions, the mobility of the ^{32}P-CVB3 1 to 250 RNA on a nondenaturing polyacrylamide gel was decreased from that of its free form (lane 1) to that of its complexed form (lane 4). The same protein(s) must be involved in the RNA-protein complexes with PV1 and CVB3 RNA since an unlabeled 1 to 246 PV1 RNA competed for complex formation with the ^{32}P-CVB3 1 to 250 RNA (lanes 5 to 7). Further evidence that the same protein(s) is involved in the complexes with PV1 and CVB3 RNA is provided in the competition experiments in which increasing amounts of unlabeled CVB3 RNA were able to compete with the PV1 RNA for complex formation (lanes 12 to 14). These results show that despite the apparent lack of conservation of the lower stem structure of stem-loop D, CVB3 5′ NCR sequences are able to form a complex with

the protein(s) in the 60%+ extract similar to the one formed with PV1 5′ NCR sequences.

The mobility shift assays and competition experiments with HRV14 RNA sequences are shown in Fig. 6B. In contrast to the PV1 or CVB3 RNA substrates, 4 μg of the 60%+ extract was not able to complex all the HRV14 RNA substrate, suggesting that the interaction of this protein(s) with an HRV14 RNA substrate is not as efficient as with the PV1 or CVB3 RNA substrate (compare Fig. 6B, lane 5, with Fig. 6A, lanes 4 and 11). As shown in lanes 6 to 8, the same protein(s) is involved in the complexes with the HRV14 RNA and PV1 RNA substrates since an increasing amount of unlabeled PV1 1 to 246 RNA competed for the complex formation with the ^{32}P-HRV14 1 to 260 RNA. Further evidence of this is shown by the ability of an unlabeled HRV14 1 to 260 RNA to compete for the complex formation with the ^{32}P-PV1 1 to 246 RNA (lanes 9 to 12). The results show that HRV14 5′ NCR sequences are also able to form a complex with the protein(s) in the 60%+ extract similar to that of PV1 5′ NCR sequences. Comparison of the ability of an HRV14 RNA substrate (Fig. 6B, lanes 9 to 12) and a CVB3 RNA substrate (Fig. 6A, lanes 12 to 14) to compete for complex formation with a ^{32}P-PV1 1 to 246 RNA substrate suggests that the 5′ NCR sequences of CVB3 and PV1 are able to interact with the cellular protein(s) more efficiently than HRV14 RNA sequences. Nevertheless, the results show the conservation of an RNA-protein interaction between 5′ NCR sequences from PV1 and CVB3, both enteroviruses, and between HRV14, a rhinovirus, and a protein(s) from a HeLa cell extract.

RNA-protein interactions within stem-loop E sequences of the 5′ NCR. The mutations which alter the nucleotide spacing between stem-loops D and E do not appear to have their primary effect on the stem-loop D RNA-protein interaction. In light of this data, it was important to determine whether there were RNA-protein interactions with stem-loop E and whether any of the mutations which alter the spacing between these two stem-loop structures have an effect on the structure of stem-loop E or RNA-protein interactions with stem-loop E. The 220 to 460 RNA utilized to investigate any protein interactions with stem-loop E was chosen because it encompasses the stem-loop E sequences from 234 to 440. A crude representation of the predicted RNA secondary structure of stem-loop E is shown in Fig. 7. This structure is taken from the model by Skinner et al. (32), which was derived from nucleotide sequence data as well as chemical and nuclease sensitivity experiments.

The conditions needed to achieve a specific RNA-protein interaction with the 220 to 460 RNA are shown by the data presented in Fig. 8. The mobility of the ^{32}P-PV1 220 to 460 RNA alone in binding buffer is shown in lane 1. The addition of a HeLa cell protein extract to the binding reaction in the absence of any nonspecific competitor (lane 2) or in the presence of 7.5 μg of poly(dI-dC) (lanes 3) or 11 μg of tRNA (lane 4) resulted in the majority of the RNA remaining in the well with a small amount migrating as a slowly moving smear. Heparin, a negatively charged polymer, is known to reduce the nonspecific binding of proteins to RNA (3, 16). With the addition of heparin at 0.5 mg/ml after the binding reaction (lane 5), there appeared to be three distinct complexes formed. One complex ran as a more slowly migrating species (marked by HC for high complex), while the other two complexes ran close together as faster-migrating species (marked by LC for low complex). At 0.5 mg/ml, heparin appeared to reduce much of the nonspecific RNA-protein interactions which the amounts of poly(dI-dC) and tRNA used could not reduce. The addition of poly(dI-dC) (lane 6) or tRNA (lane 8) to the binding reactions in the presence of 0.5 mg of heparin per ml had little, if any, effect. The data shown in lanes 7 to 10 illustrate the effect of increasing concentrations of heparin on the specificity of RNA-protein complex formation. At 5.0 mg of heparin per ml, no RNA-protein interaction corresponding to the HC complex occurred. Instead, the majority of the RNA was found in the LC complex. This suggested that the HC complex was either due to a nonspecific RNA-protein interaction of high affinity or due to a specific interaction which is not as strong as the RNA-protein interactions in the LC complex. The control reactions displayed in lanes 11 to 14 show that the proper RNA structure and the RNA-protein complex could form at the optimal temperatures for virus growth in vivo and that the mobility shifts are the result of protein(s) in the cell extract.

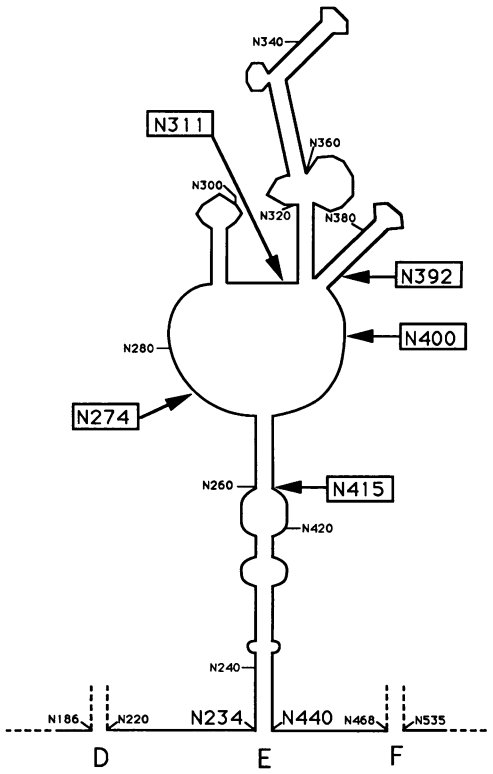

FIG. 7. Predicted RNA secondary structure of PV1 stem-loop E. This figure is a crude representation of the RNA secondary structure of stem-loop E proposed by Skinner et al. (32) which was based on data from sequence comparisons as well as chemical and nuclease sensitivity experiments (14). Nucleotide positions are indicated every 20 nucleotides (N) by the small numbers. The larger boxed numbers indicate the boundaries of RNA sequences used in competition experiments which are described in the text.

PV RNA corresponding to 220 to 460 interacts with proteins in different extracts from HeLa cells. The ^{32}P-PV1 220 to 460 RNA, encoding stem-loop E, was tested for the ability to interact with protein(s) from the various HeLa cell extracts described previously. The results from RNA mobility shift experiments with stem-loop E RNA and different protein extracts from HeLa cells are shown in Fig. 9. The data show that the stem-loop E binding activity was more concentrated in the S10 and the RSW A cut than in the 0 to 40% ammonium sulfate cut of NP-40-lysed HeLa cells, since 40

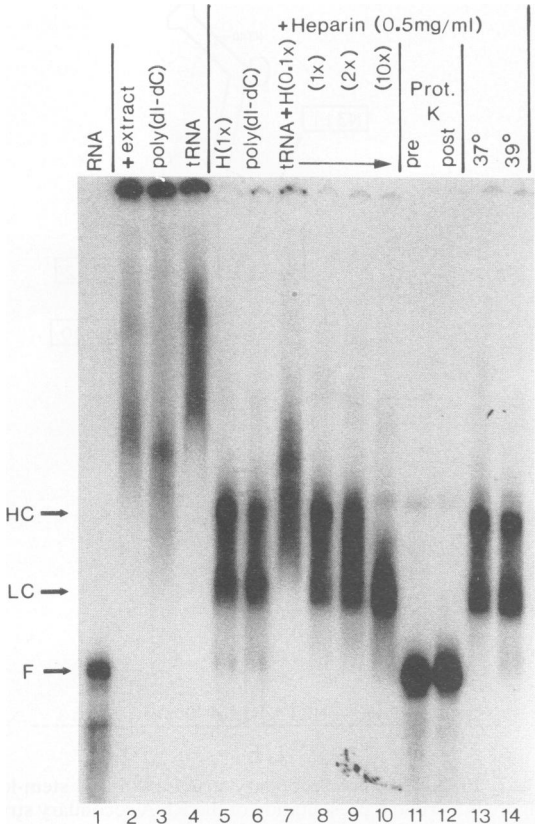

FIG. 8. Conditions for stem-loop E RNA-protein interaction. ^{32}P-PV1 220 to 460 RNA (0.5 pmol) is used in each reaction. Lane 1 contains RNA alone in buffer, and the predominant free form is marked by the F. Lanes 2 to 14 contain the ^{32}P-RNA and 70 μg of a 0 to 40% ammonium sulfate precipitation of NP-40-lysed HeLa cells (0 to 40% extract). The reaction in lane 2 contains the extract added to the RNA, while the reactions in lanes 3 and 4 also contain 7.5 μg of poly(dI-dC) and 11 μg of yeast tRNA, respectively, included in the preincubation step as nonspecific competitors. Lane 5 contains RNA and extract which has been treated with 0.5 mg of heparin per ml, and lane 6 also contains 7.5 μg of poly(dI-dC). Lanes 7 to 10 contain RNA, extract, 11 μg of yeast tRNA, and an increasing concentration of heparin from 0.05 to 5.0 mg/ml (1× = 0.5 mg/ml). Reaction conditions in lanes 11 and 12 were similar to those in lane 8 except that 25 μg of proteinase K was added to the preincubation step (lane 11) or after the binding reaction (lane 12). Reaction conditions in lanes 13 and 14 were identical to those in lane 8 except that the incubation temperatures were 37 and 39°C, respectively.

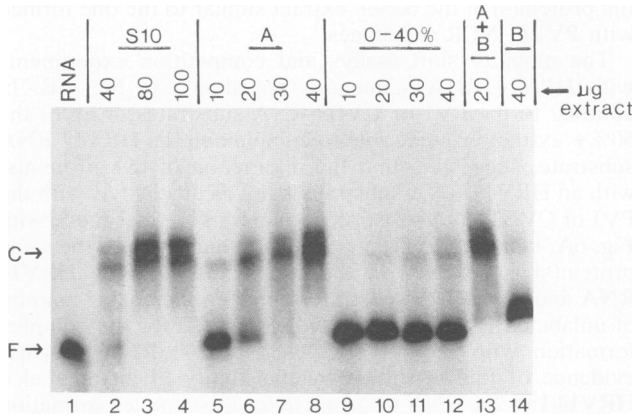

FIG. 9. Stem-loop E RNA forms a complex with protein(s) from different extracts of HeLa cells. All reactions contained 0.5 pmol of ^{32}P-PV1 220 to 460 RNA. Lane 1 displays the mobility of the free RNA (F). Reactions in all other lanes contain the indicated amounts (micrograms) of the different extracts from HeLa cells. 0–40% refers to ammonium sulfate fractions of NP-40-lysed HeLa cells, whereas A and B refer to ammonium sulfate fractions of RSW.

μg of HeLa S10 (lane 2) was able to complex at least half of the RNA and 30 μg of A cut (lane 7) was able to complex all of the RNA, while 40 μg of the 0 to 40% cut (lane 12) complexed less than half of the RNA. The greater concentration of the protein in an RSW fraction would be expected since the NP-40-lysed cellular extract represents a total cytoplasmic extract, whereas the RSW fractions are devoid of proteins present in the postribosomal supernatant as well as ribosomes. Finally, the data show that incubation of stem-loop E RNA with 40 μg of RSW B cut produced a barely detectable RNA-protein complex (lane 14). This may have been the result of a small amount of the same proteins present in the A cut since these were somewhat crude fractionations. Note that a mixture of 20 μg of both A and B cut fractions appeared to form a complex with more of the RNA than 20 μg of A cut alone (compare lane 13 with lane 10). The result may be due to some of the RNA binding activity being present in the B cut (as shown in lane 14) and not to a different RNA binding activity, since the complex formed appeared to have the same electrophoretic mobility.

Truncated 220 to 460 RNAs as competitors for proteins binding to stem-loop E. The 220 to 460 RNA used in the mobility shift assay encompasses stem-loop E, which itself consists of 206 nucleotides (Fig. 7). In an attempt to determine the sequences or structures which are necessary for the RNA-protein interaction within stem-loop E, we made a number of transcription vector constructs which encoded smaller regions of stem-loop E (described in Materials and Methods). Unlabeled (cold) RNAs from these constructs were synthesized in vitro and used in the mobility shift assay to determine their ability to compete for the formation of complexes between the ^{32}P-PV1 220 to 460 RNA and a protein(s) from HeLa cell extracts. The results from these competition experiments are displayed in Fig. 10A. The addition of unlabeled 220 to 460 RNA at a 10- and 20-fold molar excess (lanes 3 and 4, respectively) to the binding reactions shows that this RNA was able to compete for complex formation and returned the ^{32}P-PV1 220 to 460 RNA substrate to the free (F) form. An RNA from 220 to 415 was able to compete for formation of complexes nearly as well as the 220 to 460 RNA substrate (lanes 5 and 6), but when this RNA was shortened to 220 to 392, the ability to compete for formation of complexes was reduced considerably since a 40-fold molar excess (lane 8) did not compete as well as a 20-fold molar excess of the 220 to 415 RNA (lane 6). Removing sequences from the 5′ side of stem-loop E also had detrimental effects on this RNA-protein interaction as illustrated by competition with the 274 to 415 RNA (lanes 9 and 10). A 40-fold molar excess of the 274 to 415 RNA competed only approximately half as well as a 20-fold molar excess of the 220 to 415 RNA (compare lanes 10 and 6). Further truncation of the RNA to 274 to 400 (lanes 11 and 12) or 274 to 392 (lane 13) resulted in further decreases in the ability to compete for formation of complexes. Finally, RNAs from 311 to 400 (lane 14) and 311 to 415 (data not shown) showed no ability to compete for formation of

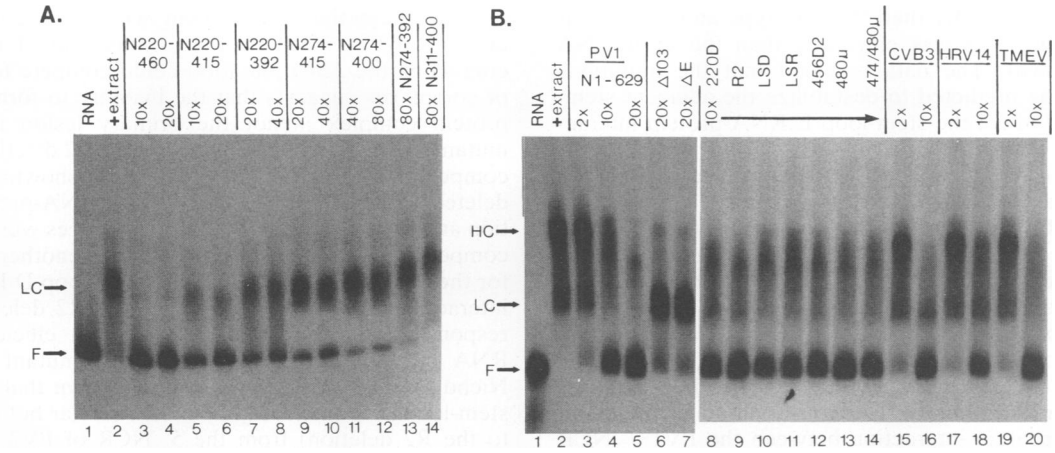

FIG. 10. Competition experiments to define the stem-loop E RNA-protein interaction. (A) Results of competition experiments with unlabeled truncated 220 to 460 RNAs as competitors to narrow down the site of interaction on the RNA substrate. All reactions in panel A contained 0.5 pmol of ^{32}P-PV1 220 to 460 RNA and 11 μg of tRNA and were treated with 5.0 mg of heparin per ml. Lanes 1 and 2 represent the mobility shift observed from the free RNA (F) to the complexed RNA (LC) upon the addition of 70 μg of the 0 to 40% extract. Lanes 3 to 14 contain 70 μg of the 0 to 40% extract and the indicated molar excess of the indicated unlabeled competitor RNAs, included in the preincubation step. (B) Results of competition experiments utilizing various 5′ NCR mutant RNAs as competitors. All reactions contained 0.5 pmol of ^{32}P-PV1 220 to 460 RNA and 11 μg of tRNA. Lanes 1 and 2 represent the mobility shift observed from free RNA (F) to complexed RNA (LC and HC, because these reactions contain only 0.5 mg of heparin per ml) upon the addition of 70 μg of the 0 to 40% extract. Lanes 3 to 20 contain 70 μg of the 0 to 40% extract and the indicated molar excess of the various unlabeled RNAs, included in the preincubation step. The 5′ NCR mutants are defined in the text. Reactions in lanes 15 to 20 contain a 2- and 10-fold molar excess of the following unlabeled RNAs added to the preincubation step: 1 to 750 CVB3 RNA (lanes 15 and 16), 1 to 628 HRV14 RNA (lanes 17 and 18), and 1 to 930 TMEV RNA (lanes 19 and 20).

complexes, even at an 80-fold molar excess. Taken together, the results from the truncated 220 to 460 competitions suggested that the minimum site of interaction with the protein(s) is ~274 to 415.

Mutant 5′ NCR RNAs as competitors for binding of proteins to stem-loop E. Our results suggested that mutations outside of stem-loop D do not have a global effect on the RNA secondary structure of the 5′ NCR (at least not on the structure of stem-loop D). It was important to also determine whether any of these mutations had an effect on the stem-loop E RNA-protein interaction. Therefore, RNAs containing mutations in other stem-loop structures (stem-loops D and F) in the PV1 5′ NCR were tested in the mobility shift assay for their ability to compete for formation of complexes with the wild-type 220 to 460 RNA substrate (refer to Fig. 1 and 5 for illustrations of the mutations and their locations within the PV1 5′ NCR secondary structure). The results from these competition experiments are shown in Fig. 10B. The results of competition experiments with RNAs containing the Δ103 and ΔE mutations showed that the stem-loop E sequences were necessary for an RNA-protein interaction and that if they were deleted from the 5′ NCR, the remaining sequences could not form an RNA-protein complex. Note that the formation of the HC complex was sensitive to competition by both of these RNAs but that formation of the LC complex was not, again suggesting that the HC complex is nonspecific and that the LC complex is specific. The competition experiments with additional competitors demonstrate that the mutant RNAs were able to compete as well as the wild-type 1 to 629 RNA (compare lanes 8 to 14 with lane 4). Decreasing the spacing between stem-loops D and E by four nucleotides (220D), deleting stem-loop D (R2), loss of the base-pairing potential of the lower stem of stem-loop D (LSD), loss of the stem-loop D RNA-protein interaction (LSD), or changing the nucleotide sequence of the lower stem of stem-loop D (LSR) does not have an effect on the stem-loop E RNA-protein interaction.

The 456D2 mutation is a deletion of nucleotides 461 and 462. Some differences exist in the RNA secondary-structure predictions in the region of the 456D2 mutation. According to one set of RNA secondary-structure predictions, nucleotides 461 and 462 would occur in a stem structure of stem-loop F (12, 27, 28). Other investigators would predict that these nucleotides are present in the single-stranded region between stem-loops E and F (32). Nevertheless, the 456D2 mutation was lethal to the recovery of infectious virus from a cDNA transfection, and RNAs containing this mutation were unable to respond at all to the translation stimulatory factors in an RSW (5, 6). Our observation that an RNA containing the 456D2 mutation could efficiently interact with the stem-loop E binding protein(s) suggested that the primary lesion of the 456D2 mutation is not the ability to form an RNA-protein complex with the stem-loop E RNA. Thus, the 456D2 mutation probably does not affect the stability of stem-loop E (if this is required for complex formation). The last two competitor RNAs contain mutations in stem-loop F and would be predicted to render a resulting virus less neurovirulent than wild-type PV1 Mahoney (15). The 480μ RNA contains a nucleotide substitution of the A at nucleotide 480 found in the neurovirulent Mahoney strain to a G as found in the attenuated Sabin strain. The 474/480μ RNA contains the mutation at nucleotide 480 as well as a base substitution at nucleotide 474 of U for the wild-type C. Both these mutations would be predicted to decrease the thermodynamic stability of the F stem-loop since the 480μ RNA would change an A · U base pair to a G · U and the 474/480μ RNA would contain the 480μ change as well as an additional G · C-to-G · U base-pair change. When translated in vitro in the mixed RRL plus HeLa S10 system, an RNA containing the 480μ mutation

translated less efficiently than the wild type and a 474/480μ RNA translated even less efficiently than the 480μ RNA (data not shown). The data revealed that the mutations which would be predicted to destabilize the adjacent stem-loop F did not affect the stem-loop E RNA-protein interaction.

Conservation of stem-loop E RNA-protein interactions among picornaviruses. In light of the earlier results that the stem-loop D RNA-protein interaction was conserved among PV1, CVB3, and HRV14 RNAs, it was of interest to determine whether the stem-loop E RNA-protein interaction was conserved as well. The results from RNA mobility shift competition experiments are shown in Fig. 10B, lanes 15 to 20. Each competitor RNA was able to compete for formation of complexes as effectively as the wild-type 1 to 629 PV1 competitor (lanes 3 and 4). The conservation of the stem-loop E RNA-protein interaction between the PV1 5′ NCR and that of the closely related enterovirus (CVB3), the slightly more distantly related rhinovirus (HRV14), and the much more distantly related cardiovirus (TMEV) suggested that the function served by this RNA-protein interaction must be important or very basic in the life cycles of these viruses and presumably to the mechanism of cap-independent internal initiation of translation.

DISCUSSION

In this report, we described two distinct interactions that occur between cellular proteins and the predicted RNA structures encoded by stem-loops D and E within the 5′ NCR of picornavirus RNA. The RNA-protein interaction between an in vitro-synthesized RNA from PV sequences 178 to 224 (i.e., stem-loop D) was first described by Najita and Sarnow (22). The data we presented in Fig. 2 showed that an RNA substrate encoding PV1 sequences 1 to 246 could form a complex with the cellular protein(s). Najita and Sarnow (22) suggested that the protein involved in this interaction was a membrane protein because their data indicated that the presence of this protein in extracts was dependent on NP-40 lysis of cells. In agreement with previous experiments (22), our results showed that the RNA binding activity fractionates to the supernatant of a 60%+ ammonium sulfate precipitation of NP-40-lysed HeLa cells. However, we found that the RNA binding activity was also present in an S10 extract from HeLa cells which was generated by Dounce homogenization of the cells in the absence of detergent. Therefore, the presence of this protein is not strictly dependent on NP-40 lysis of HeLa cells. The protein(s) does not appear to be an integral membrane protein, although it may still be a membrane-associated protein since preparation of an S10 extract probably disrupts some cellular membranes. When the supernatant from a 60%+ ammonium sulfate precipitation of an RSW was tested in an RNA mobility shift assay, the binding activity was detected (data not shown). RSW contains many known translation initiation factors necessary for cap-dependent translation and possibly novel proteins involved in cap-independent translation (since RSW stimulates PV1 translation in vitro). The presence of stem-loop D RNA binding activity in the RSW is indirect evidence that this protein (and therefore this RNA-protein interaction) is involved in a step required to stimulate cap-independent translation of PV1 RNA.

Using unlabeled RNAs as competitors in the mobility shift assay to define the RNA substrate requirements for RNA-protein interactions, we showed that the stem-loop D RNA-protein interaction could occur within the context of the entire 5′ NCR. The fact that a nucleotide 1 to 747 RNA containing the 220D mutation could compete for formation of complexes suggests that the inability to form this RNA-protein complex is not the primary lesion in the 220D mutant. A 1 to 747 RNA containing the R2 deletion could not compete for formation of complexes, showing that these deleted sequences are involved in the RNA-protein interaction and that the remaining RNA sequences were not able to compensate for the deletion by forming another binding site for the protein(s). The loss of the stem-loop D RNA-protein interaction in an RNA containing the R2 deletion may be responsible for the reduced translation efficiency of this RNA and the slower growth of the R2 mutant virus (5, 6). Nicholson et al. (23) have recently shown that deleting the stem-loop D sequences (189 to 223; similar but not identical to the R2 deletion) from the 5′ NCR of PV2 reduced the translation efficiency by ~50%. These findings confirmed our initial results on the R2 deletion.

The conservation of nucleotide sequences in stem-loop D is very striking in that sequences in the upper stem, loop, and bulge are highly conserved among PVs, coxsackieviruses, and rhinoviruses, whereas only one nucleotide, 215, in the lower stem is conserved among all PV strains (refer to Fig. 4). The LSD and LSR mutations in the lower stem were designed to directly address the question of whether maintenance of base-pairing potential in the lower stem is required for this RNA-protein interaction (Fig. 5). Our observation that the LSD mutation did not compete and the LSR mutation did compete with a wild-type RNA substrate for complex formation shows that maintenance of a base-paired structure in the lower stem is necessary for the stem-loop D RNA-protein interaction, while specific nucleotide sequences are not important. Since there is little sequence conservation in the lower stem and the LSR mutation has changed all the nucleotides (except the conserved 215) in the lower stem, the RNA binding protein(s) probably does not directly interact with the nucleotides in the lower stem. Rather, the base-paired structure is necessary to present the other nucleotides in the proper context.

The data shown in Fig. 6 demonstrated that the stem-loop D RNA-protein interaction is conserved among PV1, CVB3, and HRV14. The results with CVB3 are somewhat puzzling because the lower stem of stem-loop D is not predicted to be base paired. In addition, results of our experiments displayed in Fig. 5 showed that maintenance of a base-paired structure in the lower stem of PV1 was essential for this RNA-protein interaction. On the other hand, it is known from recombinant virus constructs that CVB3 sequences can substitute for PV1 sequences in the stem-loop D region (as well as most of the 5′ NCR) and provide the necessary functions for a virus with wild-type properties (14). These results underscore that, while there is in vivo conservation of function between the 5′ NCR of PV1 and CVB3 and in vitro conservation of the stem-loop D RNA-protein interaction, the interaction between the cellular protein(s) and CVB3 RNA must have requirements different from those for PV1. A lower stem structure is predicted to exist in stem-loop D of HRV14 as well as some sequence conservation with PV1 in the upper stem, loop, and bulge sequences. Therefore, it is not surprising that the stem-loop D RNA-protein interaction was also conserved. Recombinant constructs have not been made between the 5′ NCRs of PV1 and HRV14. In light of the conservation of this RNA-protein interaction in vitro, it would be of interest to generate such recombinant constructs in infectious cDNAs of PV1 and

assay for the conservation of function in vivo. Finally, competition experiments were performed with RNAs from the 5′ NCR of the more distantly related cardiovirus, TMEV (data not shown). TMEV encodes a 5′ NCR of ~1,100 nucleotides, and less is known about the sequences which are required for cap-independent initiation of this viral RNA. TMEV RNAs from 1 to 930 were able to compete with PV1 RNA for stem-loop D complex formation. The conservation of the stem-loop D RNA-protein interaction among four different picornaviruses is strong evidence that this interaction plays a functionally important role for all these viruses.

In this report, we described an RNA-protein interaction between the sequences encoded in stem-loop E of the PV1 5′ NCR and a cellular protein(s), an interaction not previously described. Using the RNA mobility shift assay, we discovered a specific interaction between PV1 sequences 220 to 460 and a cellular protein which fractionated to the A cut of an RSW of HeLa cells. The stem-loop E RNA binding activity was also present in the postribosomal supernatant (data not shown). The fractionation of the stem-loop E RNA binding activity to the A cut of an RSW as well as the site of interaction being within a region required for internal initiation of PV RNA is suggestive evidence that this protein is involved in translation initiation. The RSW A cut is known to contain eukaryotic initiation factors eIF-3 and eIF-4B (among others [10]), although neither of these proteins is known to possess a sequence- or structure-specific RNA binding activity.

Utilizing RNAs containing smaller regions of the stem-loop E sequences, the sequences required for RNA-protein interaction were narrowed down somewhat. Deletion of sequences on the 3′ side of the stem structure from 416 to 460 had little effect, whereas further deletion to 400 or 392 had an increasing effect on the ability of the remaining RNA to compete for formation of complexes in the RNA mobility shift assay. Deletion of sequences on the 5′ side of stem-loop E from 220 to 274 had a drastic effect on the ability of the remaining RNA to compete for formation of complexes. The results suggested that the presence of the single-stranded sequences on both sides of the large loop in the center of the stem-loop E structure and/or the ability to form the stem structure at the base of the large loop were important to maintaining the RNA-protein interaction (refer to Fig. 7). Together, these results suggest that an RNA structure from ~260 to 415 is required for the presentation of the sequences or structures which make direct contact with the protein(s), although the most effective competitor was the 220 to 415 RNA. However, from our experiments, we cannot define the site(s) of direct contact.

Results from the competition experiments utilizing unlabeled competitor RNAs containing lesions elsewhere (outside stem-loop E) in the 5′ NCR showed that mutations which perturb other stem-loop structures do not have an effect on the stem-loop E RNA-protein interaction (and presumably the structure of stem-loop E). Mutations which would disrupt (LSD), change the nucleotide sequence of (LSR), or delete (R2) stem-loop D did not affect the stem-loop E RNA-protein interaction. The mutations which would be predicted to lower the thermodynamic stability of stem-loop F (456D2, 480μ, 474/480μ), despite having severe effects on viral growth and translation in vitro, also did not appear to affect the stem-loop E RNA-protein interaction. In addition, the 220D mutation, which decreases the spacing between stem-loops D and E, did not appear to affect the stem-loop E RNA-protein interaction. Thus, the overall structure of stem-loop E and the interaction with a cellular protein(s) appears to be independent of the stability of the adjacent stem-loop structures.

The competition experiments utilizing RNAs encompassing the 5′ NCRs of CVB3, HRV14, and TMEV showed that the stem-loop E (as well as the stem-loop D) RNA-protein interaction is conserved among viruses from the enterorhinovirus group as well as a more distantly related cardiovirus. Although the sequences and structures of the regions which facilitate internal initiation of the enterovirus-rhinovirus and the cardiovirus-aphthovirus groups are quite different (12), our observation that the PV1 stem-loop D and E RNA binding activities are subject to competition by the 5′ NCR RNAs of members of each of these virus groups suggests that the function of this RNA-protein interaction in cap-independent internal initiation of translation is conserved between these two groups.

The presence of proteins that independently bind to stem-loop D and stem-loop E of PV1 RNA in a number of cell types is further evidence for conservation of some basic cellular function for these protein(s). Extracts from NGP (a human neuroblastoma cell line) and BHK-21 cells and RRL were used in the RNA mobility shift assays to test for the presence of the stem-loop D and E RNA binding activities (data not shown). Extracts from BHK-21 and NGP cells contained both RNA binding activities at concentrations roughly equal to those present in HeLa cell extracts. RRL also contained both RNA binding activities, suggesting that neither of these proteins is one of the unique factors from HeLa cells which stimulate in vitro translation of PV1 RNA. However, we have not determined whether the RNA binding activities found in HeLa extracts and RRL have the same affinity for their RNA substrates or whether these proteins are present at equivalent concentrations in each of these extracts. The presence of each of the RNA binding activities in RRL is consistent with the data showing that sequences 1 to 930 of the 5′ NCR of the cardiovirus TMEV were able to compete with PV1 sequences for formation of complexes with the stem-loop D and E RNA binding proteins present in HeLa cell extracts. TMEV RNA, like encephalomyocarditis virus RNA, is translated faithfully and efficiently in an RRL translation system and does not require the addition of HeLa cell factors (29). Results from our preliminary data showing that extracts from BHK cells, which support the growth of encephalomyocarditis virus and TMEV, also contain each of these RNA binding activities are further support for a basic, conserved role for such RNA-protein interactions in the life cycles of a number of different picornaviruses.

The results presented in this report describe RNA-protein interactions between two adjacent stem-loop structures (D and E) in the 5′ NCR of PV1 and two distinct RNA binding activities which are present in the 60%+ (C cut) and 0 to 40% (A cut), respectively, ammonium sulfate fractions of an RSW from HeLa cell extracts. Since it was shown that the primary defect in an RNA containing the 220D mutation was not the ability to form the RNA-protein complexes, then possibly a step subsequent to complex formation is the primary defect. The possibility that changing the spacing between these two stem-loop structures affects a necessary conformational change in the RNA superstructure induced by either RNA-protein or protein-protein interactions (or both) is an attractive model supported by the data presented here. The purification and identification of both of these RNA binding activities will be important in understanding the mechanism of cap-independent translation of picornavirus RNAs and in possibly identifying novel cellular factors involved in cap-independent translation of cellular mRNAs.

ACKNOWLEDGMENTS

We are indebted to Hung Nguyen for providing suspension cultures of HeLa and NGP cells. We thank Wing Kong and Raymond Roos for a gift of protein extract from BHK-21 cells. We also thank Aurelia Haller for comments on the manuscript.

This research was supported by Public Health Service grant AI26765 from the National Institutes of Health and by core support from the Cancer Research Institute, University of California, Irvine.

REFERENCES

1. **Borovjagin, A. V., A. G. Evstafieva, T. Y. Ugarova, and I. N. Shatsky.** 1990. A factor that specifically binds to the 5'-untranslated region of encephalomyocarditis virus RNA. FEBS Lett. **261**:237–240.
2. **Brown, B. A., and E. Ehrenfeld.** 1979. Translation of poliovirus RNA *in vitro*: changes in cleavage pattern and initiation sites by ribosomal salt wash. Virology **97**:396–405.
3. **Cheng, S.-C., and J. Abelson.** 1987. Spliceosome assembly in yeast. Genes Dev. **1**:1014–1027.
4. **del Angel, R. M., A. G. Papavassiliou, C. Fernández-Tomás, S. J. Silverstein, and V. R. Racaniello.** 1989. Cell proteins bind to multiple sites within the 5' untranslated region of poliovirus RNA. Proc. Natl. Acad. Sci. USA **86**:8299–8303.
5. **Dildine, S. L., and B. L. Semler.** 1989. The deletion of 41 proximal nucleotides reverts a poliovirus mutant containing a temperature-sensitive lesion in the 5' noncoding region of genomic RNA. J. Virol. **63**:847–862.
6. **Dildine, S. L., K. R. Stark, A. H. Haller, and B. L. Semler.** 1991. Poliovirus translation initiation: differential effects of directed and selected mutations in the 5' noncoding region of viral RNAs. Virology **182**:742–752.
7. **Dorner, A. J., B. L. Semler, R. J. Jackson, R. Hanecak, E. Duprey, and E. Wimmer.** 1984. In vitro translation of poliovirus RNA: utilization of internal initiation sites in reticulocyte lysate. J. Virol. **50**:507–514.
8. **Earle, J. A. P., R. A. Skuce, C. S. Fleming, E. M. Hoey, and S. J. Martin.** 1988. The complete nucleotide sequence of bovine enterovirus. J. Gen. Virol. **69**:253–263.
9. **Haller, A. A., and B. L. Semler.** Submitted for publication.
10. **Helentjaris, T., E. Ehrenfeld, M. L. Brown-Luedi, and J. W. B. Hershey.** 1979. Alterations in initiation factor activity from poliovirus-infected HeLa cells. J. Biol. Chem. **254**:10973–10978.
11. **Inouye, S., and M. Inouye.** 1987. Oligonucleotide-directed site-specific mutagenesis using double-stranded plasmid DNA, p. 181–206. *In* S. A. Narang (ed.), Synthesis and applications of DNA and RNA. Academic Press, Inc., New York.
12. **Jackson, R. J., M. T. Howell, and A. Kaminski.** 1990. The novel mechanism of picornavirus RNA translation. Trends Biochem. Sci. **15**:477–483.
13. **Jang, S. K., and E. Wimmer.** 1990. Cap-independent translation of encephalomyocarditis virus RNA: structural elements of the internal ribosome entry site and involvement of a cellular 57-kD RNA-binding protein. Genes Dev. **4**:1560–1572.
14. **Johnson, V. H., and B. L. Semler.** 1988. Defined recombinants of poliovirus and coxsackievirus: sequence-specific deletions and functional substitutions in the 5'-noncoding regions of viral RNAs. Virology **162**:47–57.
15. **Kawamura, N., M. Kohara, S. Abe, T. Komatsu, K. Tago, M. Arita, and A. Nomoto.** 1989. Determinants in the 5' noncoding region of poliovirus Sabin 1 RNA that influence the attenuation phenotype. J. Virol. **63**:1302–1309.
16. **Konarska, M. M.** 1989. Analysis of splicing complexes and small nuclear ribonucleoprotein particles by native gel electrophoresis. Methods Enzymol. **180**:442–453.
17. **Konarska, M. M., and P. A. Sharp.** 1986. Electrophoretic separation of complexes involved in the splicing of precursors to mRNA. Cell **46**:845–855.
18. **Lawson, M. A.** 1991. Ph.D. thesis. University of California, Irvine.
19. **Luz, N., and E. Beck.** 1990. A cellular 57 kDa protein binds to two regions of the internal initiation site of foot-and-mouth disease virus. FEBS Lett. **269**:311–314.
20. **Meerovitch, K., J. Pelletier, and N. Sonenberg.** 1989. A cellular protein that binds to the 5'-noncoding region of poliovirus RNA: implications for internal translation initiation. Genes Dev. **3**:1026–1034.
21. **Mizutani, S., and R. J. Colonno.** 1985. In vitro synthesis of an infectious RNA from cDNA clones of human rhinovirus type 14. J. Virol. **56**:628–632.
22. **Najita, L., and P. Sarnow.** 1990. Oxidation-reduction sensitive interaction of a cellular 50-kDa protein with an RNA hairpin in the 5' noncoding region of the poliovirus genome. Proc. Natl. Acad. Sci. USA **87**:5846–5850.

22a. **Nguyen, H., and B. L. Semler.** Unpublished data.

23. **Nicholson, R., J. Pelletier, S.-Y. Le, and N. Sonenberg.** 1991. Structural and functional analysis of the ribosome landing pad of poliovirus type 2: in vivo translation studies. J. Virol. **65**:5886–5894.
24. **Pelletier, J., G. Kaplan, V. R. Racaniello, and N. Sonenberg.** 1988. Translation efficiency of poliovirus mRNA: mapping of inhibitory *cis*-acting elements within the 5' noncoding region. J. Virol. **62**:2219–2227.
25. **Pelletier, J., G. Kaplan, V. R. Racaniello, and N. Sonenberg.** 1988. Cap-independent translation of poliovirus mRNA is conferred by sequence elements within the 5' noncoding region. Mol. Cell. Biol. **8**:1103–1112.
26. **Pelletier, J., and N. Sonenberg.** 1988. Internal initiation of translation of eukaryotic mRNA directed by a sequence derived from poliovirus RNA. Nature (London) **334**:320–325.
27. **Pilipenko, E. V., V. M. Blinov, L. I. Romanova, A. N. Sinyakov, S. V. Maslova, and V. I. Agol.** 1989. Conserved structural domains in the 5'-untranslated region of picornaviral genomes: an analysis of the segment controlling translation and neurovirulence. Virology **168**:201–209.
28. **Rivera, V. M., J. D. Welsh, and J. V. Maizel.** 1988. Comparative sequence analysis of the 5' noncoding region of the enteroviruses and rhinoviruses. Virology **165**:42–50.
29. **Roos, R. P., W.-P. Kong, and B. L. Semler.** 1989. Polyprotein processing of Theiler's murine encephalomyelitis virus. J. Virol. **63**:5344–5353.
30. **Roos, R. P., S. Stein, Y. Ohara, J. Fu, and B. L. Semler.** 1989. Infectious cDNA clone of the DA strain of Theiler's murine encephalomyelitis virus. J. Virol. **63**:5492–5496.
31. **Sarnow, P.** 1989. Translation of glucose-regulated protein 79/immunoglobulin heavy-chain binding protein mRNA is increased in poliovirus-infected cells at a time when cap-dependent translation of cellular mRNAs is inhibited. Proc. Natl. Acad. Sci. USA **86**:5795–5799.
32. **Skinner, M. A., V. R. Racaniello, G. Dunn, J. Cooper, P. D. Minor, and J. W. Almond.** 1989. New model for the secondary structure of the 5' non-coding RNA of poliovirus is supported by biochemical and genetic data that also show that RNA secondary structure is important in neurovirulence. J. Mol. Biol. **207**:379–392.
33. **Tabor, S., and C. C. Richardson.** 1987. DNA sequence analysis with a modified bacteriophage T7 DNA polymerase. Proc. Natl. Acad. Sci. USA **84**:4767–4771.
34. **Trono, D., R. Andino, and D. Baltimore.** 1988. An RNA sequence of hundreds of nucleotides at the 5' end of poliovirus RNA is involved in allowing viral protein synthesis. J. Virol. **62**:2291–2299.
35. **Trono, D., J. Pelletier, N. Sonenberg, and D. Baltimore.** 1988. Translation in mammalian cells of a gene linked to the poliovirus 5' noncoding region. Science **241**:445–448.
36. **Ypma-Wong, M. F., P. G. Dewalt, V. H. Johnson, J. G. Lamb, and B. L. Semler.** 1988. Protein 3CD is the major poliovirus proteinase responsible for cleavage of the P1 capsid precursor. Virology **166**:265–270.
37. **Zhang, H., R. Scholl, J. Browse, and C. Sommerville.** 1988. Double strand DNA sequencing as a choice for DNA sequencing. Nucleic Acids Res. **16**:1220.